17th World Conference on Nondestructive Testing, 25-28 Oct 2008, Shanghai, China

Method for three-dimensional evaluation and visualization of the distribution of fibres in glass-fibre reinforced injection molded parts by µ-X-ray computed tomography

Franz PFEIFER [1], Johann KASTNER [1], Rotraud FREYTAG [2]

[1] University of Applied Sciences Upper Austria, Stelzhammerstrasse 23, 4600 Wels, Austria

[2] Transfercenter für Kunststofftechnik GmbH, Franz-Fritsch-Strasse 11, 4600 Wels, Austria

Abstract

Glass-fibre reinforced polymer matrix composites exhibit superior properties to traditional materials. Thus, they have found a broad variety of applications in modern industry. For process development and quality control sophisticated three-dimensional methods for non-destructive characterization are needed. X-ray computed tomography (CT) is a powerful radiographic non-destructive-testing method to locate and size volumetric details in three dimensions.

This paper comprises the characterization of short glass-fibre reinforced injection molded polymeric parts by µ-CT to measure lengths and in particular the three-dimensional orientation of the fibres. To measure a maximum of sample volume the µ-CT-measurements were performed with resolutions close to the diameter of the fibres. The CT-data were processed by various three-dimensional filters such as anisotropic diffusion, threshold and thinning operations. The anisotropic diffusion filter leads to better contrast between fibres and the polymeric matrix. Therefore, the individual fibres can be extracted by thresholding and the medial axis of every fibre can be determined by a thinning algorithm. From these data fibre lengths and the three-dimensional orientation can be determined. The final result of the CT-evaluation procedure is a three-dimensional representation and visualization of the fibre distribution by means of color coded vector-fields and glyphs.

In addition, the experimental CT-results were compared to simulation results of the injection molding process using Moldflow. The differences between the CT-results and the simulation are visualized and analyzed in three dimensions by means of the orientation tensor. The CT-results correspond to the calculated fibre orientation in the injection molded part quite well.

Keywords: computed tomography, fibre reinforced polymer, data evaluation, orientation tensor

1. Introduction

Polymer fibre composites have an increased stiffness and increased strength to weight ratio compared to metallic and other “traditional” materials. Therefore the applications of these materials become more and more important in modern industry [1]. Non-destructive and contact-free techniques for the 3D-characterisation of fibre composites face an increasing demand in process development and production. Computed tomography (CT) is a radiographic NDT-method to locate and size volumetric details in three dimensions [2, 3, 4]. Due to measurement speed and quality, XCT systems with cone beam geometry and matrix detectors have gained general acceptance in materials science. Using CT, a specimen is placed on a rotary plate between the X-ray source and the detector. The specimen is rotated step by step, taking a projection image at each angular position. A computer cluster reconstructs the penetration images to a volume dataset. At each position of the resulting dataset a grey-value is calculated, which corresponds to the spatial X-ray attenuation coefficient.

We report on a workflow to extract the individual fibres out of the CT-data. This workflow consists of 5 major steps as shown in Fig. 1. From the extracted fibres the orientation tensor for a selected volume is calculated. Additionally, the experimental results are compared to simulation results of the injection moulding process using *Moldflow Plastic Insight[5]*.

2. Experimental

A common glass fibre reinforced polymer sample was investigated - PBT-polybutylene terephthalate with 10 % and 30 % glass fibre content. The mean fibre diameter was 20 µm and the mean fibre length 0.1 mm. The samples were prepared by injection moulding on an Engel injection moulding machine. The orientation of the glass fibres in the injection moulded parts was calculated by using Moldflow MPI 6.1 [5] by TCKT GmbH. The X-ray tomograms were scanned at a Rayscan 250E CT-device constructed by Wälischmiller Inc with a 225 keV micro focus tube and a 1024x1024 a-Si flat panel matrix-detector [2,4]. The actual x-ray energy used was in the range between 160-200 keV. The tube current and the magnification were selected in a way, that the resolution of the whole system was 8.6 µm.

3. 3D-Image Processing and CT-data evaluation

3.1 General Issues

Compared to two-dimensional image data, three-dimensional datasets offer the possibility to analyze more data. Consequently, the key figures calculated from these datasets provide more significance than those calculated from two-dimensional datasets. Nevertheless, this gain in significance is on cost of runtime needed to analyze the datasets. Furthermore, many 2D image processing routines do not easily expand into three dimensions. CT-datasets contain a high level of noise portion which has to be eliminated, moreover, the number of volume elements (voxels) which represent a fibre is due to the limited resolution very limited. To overcome these problems suitable image processing techniques have to be chosen.

The following sections will describe the image processing techniques used to extract the fibres as well as the calculation of the three-dimensional orientation tensor and the visualization of the differences between simulated and experimental data. The workflow for CT-data evaluation is based on the work of J.C. Tan et al [6]. It is shown in Figure 1.

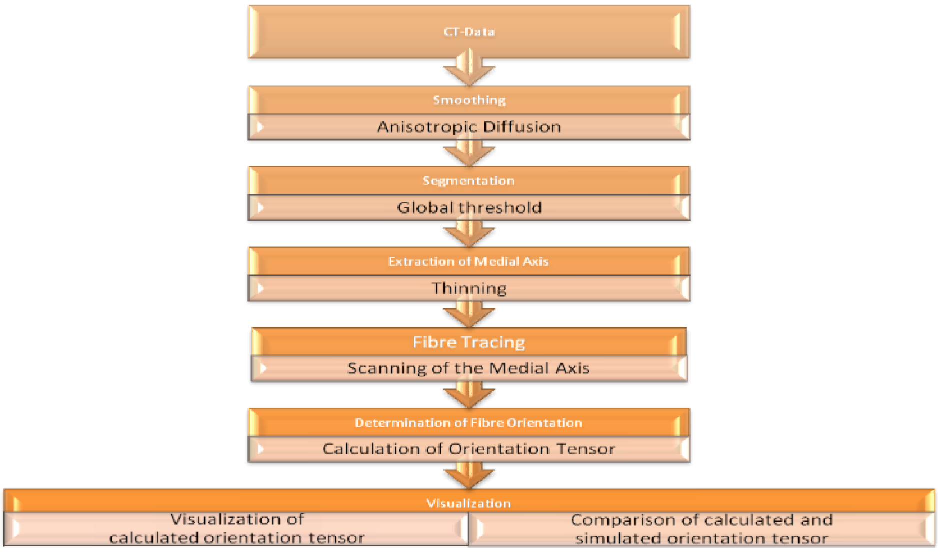

Figure 1: The workflow of the 3D-CT data analysis to extract the fibres and calculate the orientation tensor.

3.2 Pre-Processing and Segmentation

The quality of the CT-data makes it hard to separate the fibres from the surrounding polymer matrix due to noise. In general, noise in image data is eliminated by the use of smoothing filters like Gaussian smoothing, Mean or Median filters[7]. The disadvantage of these filters is that regions with high intensity differences are smoothed as well, leading to a loss of information concerning the fibre edges. Therefore, the data is smooth using Perona and Shiota anisotropic diffusion filter[8] which does not smooth regions with high gradient magnitudes. This enables a separation of the fibres from the polymer matrix by using a simple threshold operation.

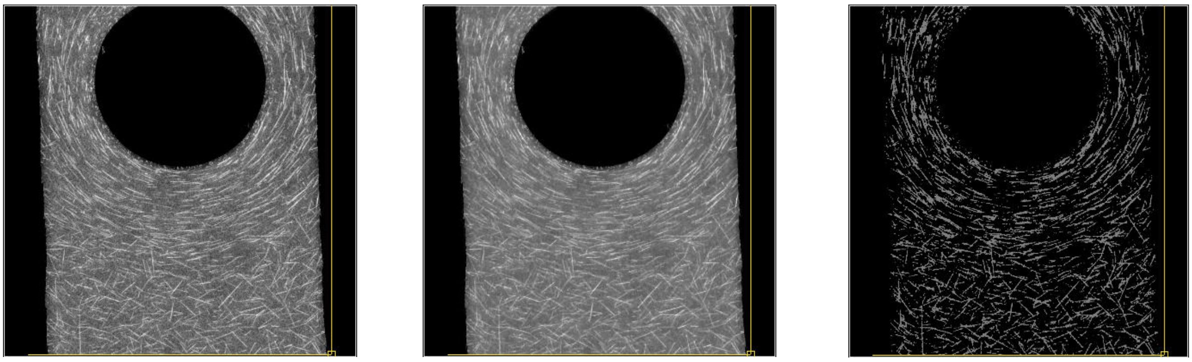

(a) (b) (c)

Figure 2: The original CT- image data (a), the smoothed image data using anisotropic diffusion (b) and the segmented fibres (c).

Figure 2 shows the results of the pre-processing step. Figure 2.a shows the original image containing noise. Nevertheless, the fibres can be recognized very well. The results of the anisotropic diffusion can be seen in Figure 2.b. As it can be seen from this image, most of the noise has been removed. Figure 2.c shows the result after applying a global threshold. It clearly can be recognized that most of the fibres have been extracted. Nevertheless some spots and sparkles are still in the image which will be removed during the fibre tracing. The output of this pre-processing step is used by a skeletonization operation.

3.3 Skeletonization

Skeletonization is a process which reduces a geometrical object to its medial axis[9]. Skeletonization, or also thinning, is used in a variety of fields of application, i.e. in medical image processing thinning can be used to extract a vessel tree. The thinning process continuously deletes border points of an object until only the medial axis of an object remains. Though, topological and geometrical constraints must be satisfied, which are to preserve the number of connected objects, cavities and holes in the original shape. Generally spoken the skeletonization process examines the local connectivity of a voxel. While only 256 possible neighbourhood configurations have to be check in two-dimensional images, the number of possible neighbourhood configurations increases to 67, 108, 864 in three-dimensional images leading to a significant increase in runtime.

3.4 Fibre Tracing

The output of the thinning process is used to trace the fibres. Therefore, additional checks have to be made. As fibres can touch, so called clusters are created. A cluster is defined as a voxel having more than two neighbours. Figure 3, (a) and (b), shows two possible configurations of a cluster. The shaded voxels are the centre of the cluster. To determine the centre voxels the neighbourhood of each voxel is examined. As it can be seen from Figure 3, a and b, the voxels left and right of the centre voxels are neighbours of the voxel on top of the centre too which would make them to centre candidates. This voxels are called to be mixed adjacent. To check this mixed adjacency three rules are introduced. Two voxels p and q are called mixed adjacent, if

$$q \in N_6 \text{, or} \tag{1}$$

$$q \in N_{18} \vee N_6(q) \cap N_6(p) = \{\} \text{, or} \tag{2}$$

$$q \in N_D \vee N_6(q) \cap N_6(p) = \{\} \vee N_{18}(q) \cap N_{18}(p) = \{\} . \tag{3}$$

Applying these rules with the neighbourhood configurations shown in Figure 3 c-f to all the voxels in the skeleton which have more than two neighbours leads to the identification of all clusters. These clusters are stored in a hash map for further processing.

The fibre tracing routine uses the cluster information to extract the path segments of fibres. Therefore, this routine traces a fibre from the beginning to its end or if a cluster is reached. Segments which are not part of a cluster and whose length is less than a user specified value are deleted, because it can be assumed that this fibres result from noise in the input image. After all segments are extracted, all path segments are assembled to fibres by analyzing the clusters they belong to. Therefore, the angles between each path segment of a cluster are determined. By comparing these angels it can be detected which path segments represent a fibre.

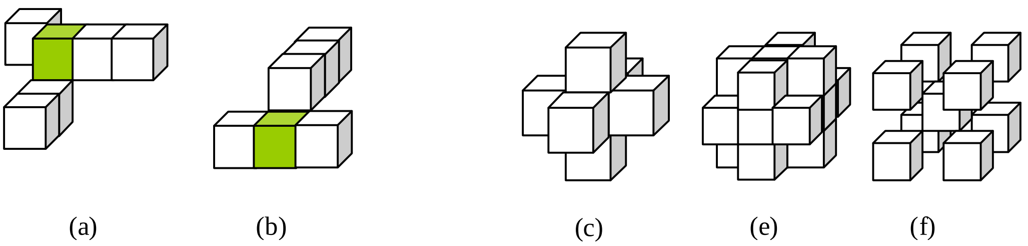

Figure 3: Two possible configurations of a cluster. The shaded voxels are the center of the cluster, (c), (e), (f): the layout of the used neighbourhood configurations (N_6, N_{18}, N_D).

3.5 Orientation tensor

Based on the extracted fibres, the three-dimensional orientation tensor[10] is calculated. Generally, the spatial orientation of a fibre is defined by the spherical coordinates r, θ, φ, where

$$r \geq 0 \text{ is the distance from the origin to a given point } k, \tag{4}$$

$$0 \leq \theta \leq \pi \text{, and} \tag{5}$$

$$0 \leq \varphi \leq 2\pi . \tag{6}$$

The spherical coordinates can be obtained from the Cartesian coordinates by:

$$r = \sqrt{x^2 + y^2 + z^2} \tag{7}$$

$$\theta = \arccos\left(\frac{z}{\sqrt{x^2 + y^2 + z^2}}\right) \tag{8}$$

$$\varphi = \arctan\left(\frac{y}{x}\right) \tag{9}$$

Additionally, a unit vector *p* which lies parallel to the fibre can be used to describe the orientation, whereas *p* is defined as follows:

$$p = \begin{pmatrix} \sin\theta\cos\phi \\ \sin\theta\sin\phi \\ \cos\theta \end{pmatrix} \qquad (10)$$

The orientation of a group of n fibres is described by the orientation tensor *which* is calculated by the dyadic product of each single fibre:

$$a_{ij} = \frac{1}{n}\sum_{k=1}^{n} a_{ij}^{k} = \frac{1}{n}\left(\sum_{k=1}^{n} p_i^k p_j^k\right) = \begin{pmatrix} a_{11} & a_{12} & a_{13} \\ a_{21} & a_{22} & a_{23} \\ a_{31} & a_{32} & a_{33} \end{pmatrix} \qquad (11)$$

The matrix diagonal components a_{11}, a_{22}, a_{33} give information about the strength of orientation in the corresponding directions. If a_{11}=1 then the fibres are oriented parallel to the x axis otherwise if a_{11}=0 then the fibres are perpendicular to the x axis. Randomly distributed fibres lead to diagonal components equal to 1/3. Moreover the sum of the matrix diagonal is always 1. The orientation tensor is often defined as a symmetrical second rank tensor which means that only six components of the orientation tensor are used:

$$\begin{pmatrix} a_{11} & a_{12} & a_{13} \\ . & a_{22} & a_{23} \\ . & . & a_{33} \end{pmatrix} \qquad (12)$$

3.6 Visualization

The whole visualization process is based on the C++ open source framework *Visualization Toolkit* (VTK)[11] which is widely used in the field of medical visualization. Besides polygon based rendering techniques, VTK supports volume rendering using *Volume Ray Casting* and *Volume Texture Mapping* techniques. To visualize the individual fibres a glyph is created according to the position and length of the fibre. The color code for each glyph is determined by extracting the Eigenvalues of the orientation tensor of the corresponding fibre (Fig. 4).

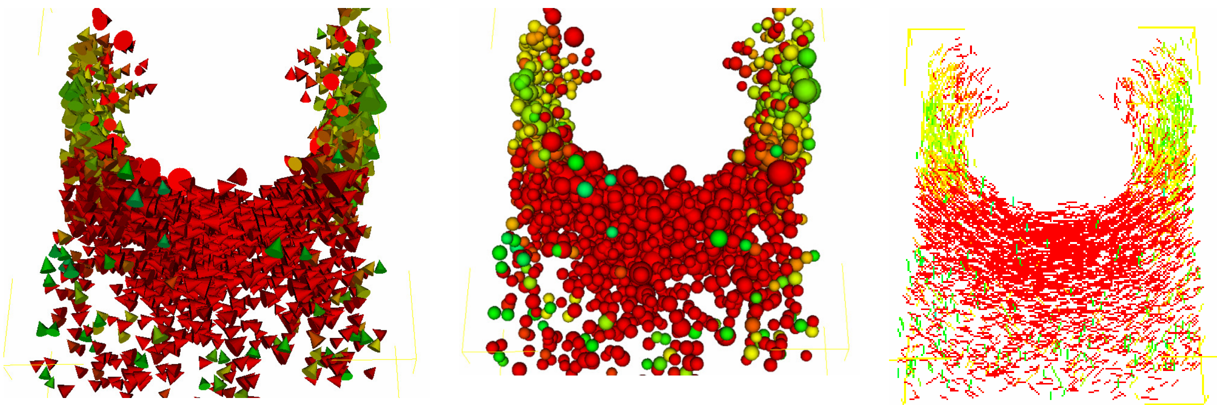

Figure 4: Visualizations of the extracted fibres using different types of glyphs. The colour corresponds to the orientation of the individual fibres

3.7 Method to compare experimental CT-results with simulated results

The main focus of this work is to enable a comparison of simulated results with experimentally obtained results. Therefore, an interface was implemented allowing comparing the simulated moulding process calculated by MoldFlow MPI with the experimentally extracted fibres. The result of the simulated moulding process is a *Finite Element Mesh* (FEM) where an orientation tensor is assigned to every cell of the FEM. To be able to compare the FEM with the extracted fibres the FEM and the CT-data have to be registered. Currently, this registration process is fully manual which will be replaced by an automatic registration method in the future. The next step is to extract the FEM-cells which lie within the bounds of the CT-data to accelerate subsequent processing steps. The next is the determination which fibres intersect which cell to extract the orientation tensor information of both, the simulated data and the experimental data. Based on the extracted orientation tensors the differences can be determined and visualized. The visualization process comprises the possibilities to visualize the FEM combined with the difference orientation tensor, or the results can be merged with the extracted fibres.

4. Results and Discussion

This section shows the results of the above described approach for a polybutylen terephthalat polymer matrix with 10 percent fibre fraction. The real part was moulded with an injection speed of 140 cm³ per second. Figure 5 shows the results of the simulation performed by MoldFlow MPI. A CT-scan was performed in the area of the bore hole in the middle of the part resulting in a dataset with a size of 767x414x884, with an isotropic voxel size of 8.6 µm.

Method	Orientation Tensors
MoldFlow MPI Orientation Tensor	$a = \begin{pmatrix} 0.519631 & 0.0489648 & 0.00149019 \\ & 0.433884 & 0.00155838 \\ & & 0.0464856 \end{pmatrix}$
Experimentally determined Orientation Tensor	$a = \begin{pmatrix} 0.392679 & 0.0188275 & 0.0156354 \\ & 0.560755 & -0.0106652 \\ & & 0.0465663 \end{pmatrix}$

Table 1: The simulated orientation tensor compared to the experimentally determined orientation tensor.

Table 1 shows the resulting orientation tensors of MoldFlow MPI and the extracted fibres in the area around the bore hole. As it can be seen the strength of orientation is highest in the x-y direction in both methods. Furthermore, it can be seen that MoldFlow MPI favours the x-direction whereas the experimentally determined orientation tensor favours the y-direction. It is noticeable, that both methods provide nearly the same value for the strength of orientation in the z-direction. Moreover it can be seen from Table 1 that the other components of the orientation tensor of the extracted fibres, with exception of the x-y component, are about 10 % higher than the simulated components.

Figure 5.a shows a visualization of the extracted fibres. Fibres with similar orientations are coloured equally. As it can be seen, the orientations of the fibres follow the shape of the bore hole very well. Figure 5.b shows visualization where the difference between the simulated and the experimentally determined orientation tensors is encoded into the colouring of the fibres. Regions with red fibres indicate big differences in the orientations, regions with green and yellow fibres indicate negligible differences.

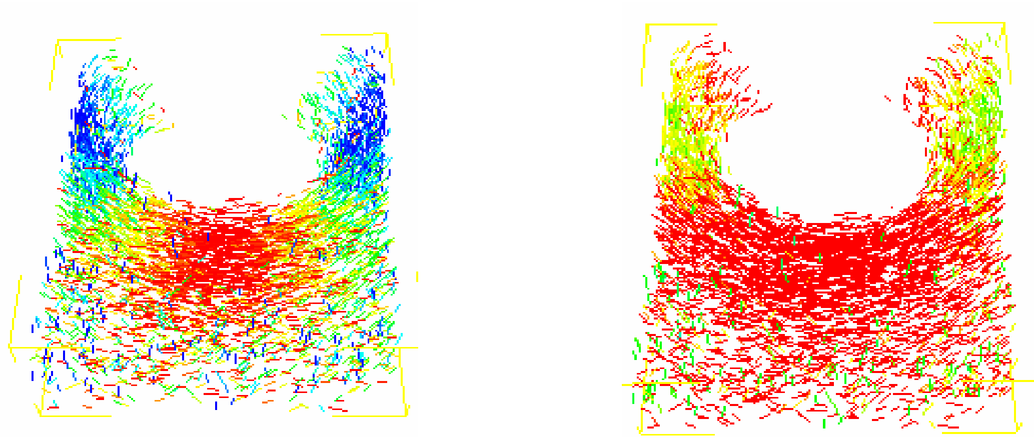

(a) (b)

Figure 5: Visualization of the experimentally determined orientation tensor (a); visualization of the differences between the simulated and experimentally determined orientation tensors (b).

5. Conclusion

Current results show that the presented approach is very promising. We have presented a workflow with 5 major steps – smoothing, segmentation, skeletonization, fibre extraction, tensor calculation – to extract the position and length of every individual fibre and to calculate the orientation tensor. The extracted fibres were visualized by colour coded glyphs. The extraction of the fibres medial axis allows the determination of many performance figures of glass-fibre reinforced injection moulded polymer parts. Furthermore, we have presented an approach for reviewing the results of a simulated injection moulding process performed with MoldFlow MPI and to compare the simulated results with the processed CT-data in 3D.

Acknowledgement

The project was supported by FH-Plus of FFG and by the government of Upper Austria.

References

[1] W. Michaeli, F.-J. Vossebürger, H. Greif und L. Wolters, „Technologie der Kunststoffe“, Carl Hanser Verlag, München, ISBN 3-446-19372-3, 2003.

[2] J. Kastner, E. Schlotthauer, P. Burgholzer and D. Stifter, “Comparison of optical coherence tomography and X-ray computed tomography for characterisation of glass-fibre polymer matrix composites”, World Conference on Nondestructive Testing, Montreal, Canada, 30. August–3. September 2004.

[3] J. Kastner (Editor), Proceedings Industrielle Computertomografietagung, Wels, Austria, 26. + 27. February 2008, ISBN 978-3-8322-6949-4, Shaker Verlag, Aachen, 2008.

[4] J. Kastner, D. Salaberger, G. Zitzenbacher, W. Stadlbauer, R. Freytag, “Determination of diameter, length and three-dimensional distribution of fibres in short glass-fibre reinforced injection moulded parts by µ-computed tomography”, Proceedings 24th annual meeting polymer processing society, Salerno, Italy, 15.-19. June 2008.

[5] www.moldflow.com/stp/english/products/mpi.htm

[6] J.C. Tan, J.A. Elliot, T.W. Clyne , “Analysis of Tomography Images of Bonded Fibre Networks to Measure Distribution of Fibre Segment Length and Fibre Orientation”, Advanced Engineering Materials 8/6, WILEY-VCH Verlag GmbH & Co KGaA, Weinheim, 2006, pp495-500.

[7] R. C. Gonzales, R. E. Woods, “Digital Image Processing”, Prentice Hall, Saddle River, New Jersey, 2002.

[8] P. Perona, A. Shiota, J. Malik, “Anisotropic diffusion – Geometry Driven Diffusion in Computer Vision”, B. M. ter Haar Romany, ed., Kluwer Academic, Boston, 1994, pp73-92.

[9] Ta-Chih Lee, Rangasami L. Kashyap, Chong-Nam Chu, “Building Skeleton Models via 3-D Medial Surface/Axis Thinning Algorithms”, Graphical Models and Image Processing 56 (6), 1994, pp438-478.

[10] A. R. Clarke, C. N. Eberhardt, “Microscopy Techniques for Material Science”, Woodhead Publishing Limited, Cambridge, 2002.

[11] William Schroeder, Ken Martin, Bill Lorensen, „The Visualization Tookit: An Object-Oriented Approach to 3-D Graphics”, Kitware Inc., 2005.